The *in vitro* and *in vivo* phosphotyrosine map of activated MuSK

Anke Watty*†, Gitte Neubauer‡, Mathias Dreger§, Manuel Zimmer*¶, Matthias Wilm‡, and Steven J. Burden*†

*Molecular Neurobiology Program, Skirball Institute, New York University Medical School, 540 First Avenue, New York, NY 10016; ‡Protein and Peptide Group, European Molecular Biology Laboratories, Meyerhofstrasse 1, 69117 Heidelberg, Germany; and §Institut für Biochemie, Fachbereich Chemie, Freie Universität Berlin, Thielallee 64, 14195 Berlin, Germany

Communicated by James C. Wang, Harvard University, Cambridge, MA, February 11, 2000 (received for review December 17, 1999)

The muscle-specific receptor tyrosine kinase MuSK plays a crucial role in neuromuscular synapse formation. Activation of MuSK is induced by agrin leading to clustering of several proteins, including acetylcholine receptors, at synaptic sites. In a first step to elucidate the signal transduction cascade following MuSK activation and leading to clustering of synaptic proteins, we sought to identify the tyrosine residues that are phosphorylated in activated MuSK. We mapped the tyrosine residues that are phosphorylated *in vitro* and *in vivo* using methods that provide high sensitivity and do not require radioactive tracers. We expressed MuSK in insect cells by using a baculovirus expression vector and mapped the tyrosines that are phosphorylated in MuSK in an *in vitro* kinase assay using matrix-assisted laser desorption ionization MS to sequence tryptic peptides fractionated by HPLC. In addition, we isolated MuSK from *Torpedo* electric organ and used nanoelectrospray tandem mass spectrometry and parent ion scanning to identify the tyrosine residues that are phosphorylated in activated, endogenous MuSK *in vivo*. We found that six of the nineteen intracellular tyrosine residues in MuSK are phosphorylated in activated MuSK: the juxtamembrane tyrosine (Y553), the tyrosines within the activation loop (Y750, Y754, and Y755), a tyrosine near the beginning of the kinase domain (Y576), and a tyrosine (Y812) within the C-terminal lobe of the kinase domain. Our biochemical data are consistent with results from functional experiments and establish a good correlation between tyrosine residues that are phosphorylated in activated MuSK and tyrosines that are required for MuSK signaling.

neuromuscular synapse | acetylcholine receptor | agrin | synapse formation | mass spectrometry

MuSK is a receptor tyrosine kinase (RTK) that is expressed selectively in skeletal muscle and has an important role in the formation of the neuromuscular junction (1, 2). Mice lacking MuSK fail to form neuromuscular synapses, fail to move or breathe, and consequently die at birth (3). Agrin, an ≈400-kDa glycoprotein that is expressed by motor neurons and deposited in the synaptic basal lamina, activates MuSK, and activation of MuSK results in the clustering of several proteins, including nicotinic acetylcholine receptors (AChR), at synaptic sites (4). Although MuSK may be associated with other proteins that participate in agrin-mediated signaling (5), activation of MuSK is necessary and sufficient to cluster AChRs (4).

Little is known about the signal transduction cascade that follows MuSK activation and ultimately leads to clustering of AChRs. RTKs initiate signaling by recruiting downstream proteins, bearing src-homology 2 (SH2) or phosphotyrosine-binding (PTB) domains, to phosphorylated tyrosine residues contained within specific recognition sequences (6). Binding of SH2 or PTB domain-containing proteins to a phosphorylated RTK often leads to phosphorylation of the recruited adapter protein and to further recruitment of components in a signal transduction cascade (6, 7).

In a first step to elucidate the signal transduction cascade that follows MuSK activation and that leads to clustering of synaptic proteins, we sought to identify the tyrosine residues that are phosphorylated in activated MuSK. We expressed MuSK in insect cells by using a baculovirus expression vector and mapped the tyrosines that are phosphorylated in MuSK in an *in vitro* kinase assay by using a matrix-assisted laser desorption ionization (MALDI) MS to sequence ^{32}P-labeled tryptic peptides fractionated by HPLC (8). In addition, we isolated endogenous MuSK from *Torpedo* electric organ and used nanoelectrospray tandem mass spectrometry and parent ion scanning to identify the phosphopeptides in activated MuSK *in vivo* (9, 10). We found that the juxtamembrane tyrosine residue (Y553), the tyrosine residues within the activation loop (Y750, Y754, and Y755), and two additional tyrosine residues within the kinase domain (Y576 and Y812) are phosphorylated in activated MuSK.

Materials and Methods

Cell Culture. Sf9 and High Five insect cells (Invitrogen) were cultured at 27°C in TMN-FH (Invitrogen) and EXCELL 400 (JRH Scientific, Lenexa, KS), respectively.

Antibodies. Antibodies to the FLAG epitope (M2) were purchased from Sigma. Antibodies to rat MuSK are directed against the carboxy-terminal 20 amino acids (CSIHRILQRMCERAEGTVGV; antibody 24908) from rat MuSK coupled to keyhole limpet hemocyanin. Antibodies to *Torpedo* MuSK are directed either against the carboxyl-terminal 20 amino acids (ASIHRILERMHQRMAAALPV; antibody 2847) coupled to keyhole limpet hemocyanin or the kinase insert region (PITARTLRPANGVGWSSGWGK; antibody 35453) (11). All antisera were produced in rabbits (Research Genetics, Huntsville, AL) and were affinity-purified with the appropriate peptide coupled to *N*-hydroxysuccinimide-activated Sepharose-4B fast flow (Pharmacia) following standard protocols (12). Secondary antibodies were purchased from Jackson ImmunoResearch.

Generation of Recombinant Baculovirus. cDNA encoding rat MuSK was cloned into the *Eco*RI and *Kpn*I restriction sites of the baculovirus transfer vector pAcSG2. The FLAG epitope was inserted into a 10-aa alternative insert in the extracellular domain of rat MuSK (13).

Recombinant baculovirus was generated by co-transfecting 2×10^6 Sf9 cells with 0.25 μg of Baculogold DNA and 2.5 μg of recombinant pAcSG2 DNA (PharMingen). After 6 days at 27°C,

Abbreviations: AChR, acetylcholine receptor; MALDI, matrix-assisted laser desorption ionization; PSD, postsource decay; PTB, phosphotyrosine binding; RTK, receptor tyrosine kinase; SH2, src-homology 2.

†To whom reprint requests should be addressed. E-mail: burden@saturn.med.nyu.edu or watty@saturn.med.nyu.edu

¶Present address: European Molecular Biology Laboratories, Meyerhofstrasse 1, 69117 Heidelberg, Germany.

The publication costs of this article were defrayed in part by page charge payment. This article must therefore be hereby marked "*advertisement*" in accordance with 18 U.S.C. §1734 solely to indicate this fact.

Article published online before print: *Proc. Natl. Acad. Sci. USA*, 10.1073/pnas.080061997. Article and publication date are at www.pnas.org/cgi/doi/10.1073/pnas.080061997

the conditioned medium was harvested, and baculoviruses were plaque-purified and amplified twice following standard protocols (PharMingen).

Expression, Affinity Purification, and *in Vitro* Phosphorylation of MuSK from High Five Cells. High Five cells were grown to 70% confluence and were infected with recombinant baculovirus. The cells ($\approx 4 \times 10^7$) were harvested after 3 days at 27°C, were washed twice with ice-cold PBS, and were lysed with chilled lysis buffer (20 mM Hepes, pH 7.4/150 mM NaCl/1 mM EDTA/1% Nonidet P-40/10 μg/ml leupeptin/10 μg/ml aprotinin/10 μg/ml pepstatin/1 mM PMSF/1 mM Na_3VO_4/10 mM NaF). The lysates were centrifuged (16,000 $\times$ *g*, 20 min, 4°C) in a tabletop centrifuge, and MuSK was immunoprecipitated with anti-FLAG affinity gel or with antibodies to MuSK (24908) and Protein A-agarose (Roche Molecular Biochemicals). The beads were washed four times with ice-cold lysis buffer and once with kinase buffer (20 mM Hepes, pH 7.4/10 mM $MnCl_2$); [γ-^{32}P]ATP (NEN) was added to the kinase buffer (20–30 μl) at a final concentration of 200 μM (2–5 μCi/nmol ATP), and the reaction was allowed to proceed for 30–90 min at room temperature. The bound proteins were eluted from the beads with SDS/PAGE sample buffer. In some experiments, MuSK was eluted from the anti-FLAG affinity gel with acidic pH: after the kinase reaction, the beads were washed once with lysis buffer and twice with 100 mM glycine (pH 5.0), and bound proteins were eluted with 0.1 M glycine (pH 2.5).

***In Vivo* Labeling of Insect Cells with [^{32}P]Orthophosphate.** High Five cells were infected with recombinant baculovirus for 3 days and were washed with labeling medium (10 mM Mes, pH 6.2/55 mM KCl/11 mM $MgCl_2$/11 mM $MgSO_4$/4 mM $NaHCO_3$/4 mM D-glucose/78 mM sucrose). [^{32}P]Orthophosphate (NEN) was added to a final concentration of 0.33 mCi/ml (1–2 mCi per 175-cm^2 flask), and the cells were incubated for 3 h at 27°C. Cells were lysed, and MuSK was immunoprecipitated as described above.

Immunoprecipitation of MuSK from *Torpedo* Electric Organ. Frozen electric organ (100 g) from *Torpedo californica* (Winkler Enterprises, San Pedro, CA) was homogenized in a Waring blender in solution A (40 mM Tris, pH 7.4/150 mM NaCl/1 mM EDTA/10 μg/ml leupeptin/10 μg/ml aprotinin/10 μg/ml pepstatin/1 mM PMSF/1 mM Na_3VO_4/10 mM NaF; 1 ml of buffer per gram of tissue). After centrifugation of the homogenate (1,800 $\times$ *g*, 10 min, 4°C), the pellet was discarded, and the supernatant was recentrifuged (35,000 $\times$ *g*, 60 min, 4°C). The pellet was resuspended in solution A containing 1% Triton X-100 and was centrifuged (35,000 $\times$ *g*, 60 min). MuSK was immunoprecipitated from the supernatant with antibody 2847 or antibody 35453 and protein A-agarose. The beads were washed four times with lysis buffer, and bound proteins were eluted with SDS/PAGE sample buffer.

SDS/PAGE, Autoradiography, and Western Blotting. Proteins were fractionated in polyacrylamide gels (14) and were transferred to nitrocellulose (Amersham) by semidry blotting. MuSK was detected with antibodies 24908 (rat) or 2847 (*Torpedo*) and horseradish peroxidase-coupled anti-rabbit antibodies by using ECL (NEN). Nonradioactive phosphorylation was detected with the mouse monoclonal antibody 4G10 (Upstate Biotechnology, Lake Placid, NY), and radioactive phosphorylation was detected by autoradiography or with a PhosphorImager (Molecular Dynamics).

Tryptic Digests in Gel and in Solution. Gel pieces from four to nine lanes of a Coomassie-stained gel were pooled, and proteins within the gel slice were reduced, alkylated, and digested with trypsin as described (15).

Tryptic digests in solution were carried out after elution of immunoprecipitated MuSK from the anti-FLAG affinity gel by acidic pH as described above. The pH was adjusted to 8–9, and trypsin (Sigma) was added at a ratio of 1/50 (wt/wt). After overnight incubation at 37°C, a second aliquot of trypsin was added, and the samples were incubated a further 5 h.

HPLC Separation of Tryptic Peptides. Tryptic peptides were separated by reverse phase-HPLC (Waters) using a C18 column (5-μm particle size, 300-Å pore size, 2.1- $\times$ 250-mm column dimensions) (Vydac, Hesperia, CA). Solution A was 0.1% trifluoroacetic acid in water, solution B was 0.085% trifluoroacetic acid in acetonitrile, and the flow rate was 0.3 ml/min. The peptides were eluted with a linear gradient of 0.4%/min from 2% solvent B to 30% solvent B and 1.9%/min from 30% solvent B to 90% solvent B. The elution profile was monitored at 215 nm with a spectrophotometer, and the radioactivity was determined by counting the Czerenkov radiation.

MALDI Time-of-Flight Mass Spectrometry. The radioactive HPLC fractions were lyophilized and resuspended in 2 μl of 50% acetonitrile/0.1% trifluoroacetic acid and were mixed 1:1 with matrix solution containing 50% acetonitrile/0.1% trifluoroacetic acid saturated with α-cyano-4-hydroxycinnamic acid. A sandwich sample preparation was used to facilitate the acquisition of postsource decay (PSD) spectra: First, a fast evaporation matrix layer containing α-cyano-4-hydroxycinnamic acid and nitrocellulose (15) was produced on the MALDI target, and 0.7 μl of the matrix/analyte mixture was spotted on this layer. This procedure results in a homogenous matrix/analyte layer consisting of very small crystals and an even distribution of the analyte throughout the sample layer.

MALDI time-of-flight MS was performed on a Bruker Reflex mass spectrometer (Bruker Daltonik, Bremen, Germany) equipped with a nitrogen laser, a reflectron, and an ion gate and operating with continuous extraction. Calibration was performed externally by using angiotensin II (Sigma) and adrenocorticotropic hormone (Sigma). PSD spectra were obtained by using the FAST method (Bruker Daltonik, Bremen, Germany).

Nanoelectrospray Mass Spectrometry. The tryptic peptide mixture was taken up in 1 μl of 80% formic acid and was diluted quickly to 15 μl with water. For the desalting step, a pulled glass capillary was filled with Poros oligoR3 sorbent to a bed volume of $\approx$100 nl and was equilibrated with 0.5% formic acid. The peptide mixture was applied and washed with 0.5% formic acid. The peptides were eluted in a stepwise fashion with about 1 μl each of 20% methanol, 50% methanol, and 50% methanol/5% ammonia directly into the spraying needle of the nanoelectrospray ion source. Each fraction was analyzed individually as described (10, 16) on an API III triple quadrupole mass spectrometer (Perkin–Elmer Sciex, Thornhill, Canada). Q1 scans were acquired with a step width of 0.1 atomic mass units and a dwell time of 1 ms. For parent and product ion scans, a step width of 0.2 atomic mass units and a dwell time of 3 ms were used. The collision gas was argon at a collision gas thickness of $\approx 3 \times 10^{14}$ molecules/cm^2. The collision energy setting for parent ion scans was 50 V (difference between R0 and R2 potentials on the API III instrument); for product ion scans, it was adjusted individually for each experiment.

Results

The intracellular sequence of mammalian MuSK contains 19 tyrosine residues, 17 of which are within the kinase domain and two of which are within the juxtamembrane region. In a first series of experiments, we expressed MuSK in insect cells and identified the tyrosine residues in MuSK that are phosphorylated in an *in vitro* kinase reaction. In a second series of experiments, we labeled the MuSK-expressing insect cells with ^{32}P-

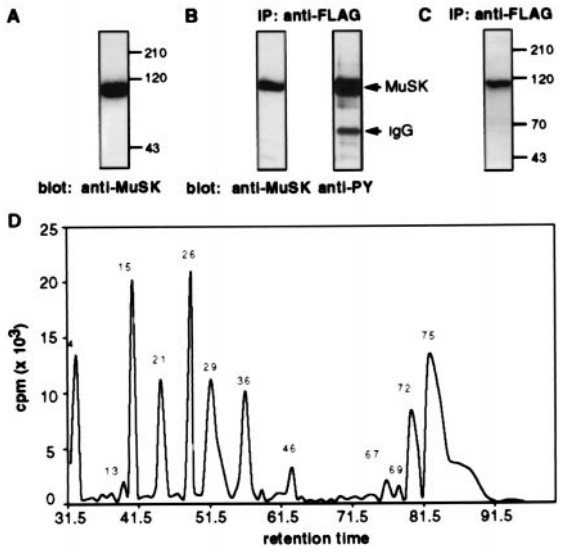

Fig. 1. *In vitro* phosphorylation and tryptic digest of MuSK expressed in insect cells. (*A*) Proteins from insect cells infected with recombinant baculoviruses encoding MuSK were separated by SDS/PAGE, and Western blots were probed with antibodies (24908) to MuSK. (*B*) MuSK was immunoprecipitated with antibodies to the FLAG epitope, and Western blots were probed with antibodies (24908) to MuSK or to phosphotyrosine (PY, 4G10). (*C*) An autoradiograph of MuSK immunoprecipitated and phosphorylated in an *in vitro* kinase assay shows that MuSK is the major if not the only protein phosphorylated in the *in vitro* kinase reaction. (*D*) Radioactivity profile of HPLC-separated tryptic peptides after *in vitro* phosphorylation and in-gel digest. Tryptic peptides were separated on a C18 column, and all radioactive fractions were analyzed by MALDI MS as summarized in Table 1.

orthophosphate and mapped the tyrosine residues in MuSK that are phosphorylated *in vivo*. In a third series of experiments, we isolated MuSK from *Torpedo* electric organ and identified the tyrosine residues that are phosphorylated in endogenous MuSK by immunoprecipitating activated MuSK from the electric organ of *Torpedo californica* and identifying phosphotyrosine residues from tryptic digests by parent ion scans by using a nanoelectrospray MS (10, 16, 17).

Expression of MuSK in Insect Cells. To identify tyrosine residues that are phosphorylated *in vitro*, we expressed MuSK in High Five cells. We immunoprecipitated FLAG-tagged MuSK (20–80 μg) from insect cells infected with recombinant baculovirus. Immunoprecipitated MuSK was phosphorylated in an *in vitro* kinase reaction containing [γ-^{32}P]ATP and $MnCl_2$. The high concentration of [γ-^{32}P]ATP included in the *in vitro* kinase reaction ensures that phosphorylation of tyrosine residues occurs at high stoichiometry and increases the probability of detecting tyrosine residues that may be minor phosphorylation sites *in vivo* but important for the biological function of the protein. Because MuSK is ^{32}P-labeled *in vitro* only after immunoprecipitation, the *in vitro* assay also minimizes the probability of detecting phosphorylation of MuSK catalyzed by other kinases.

Fig. 1 shows that MuSK is expressed in insect cells and that immunoprecipitated MuSK is tyrosine phosphorylated in insect cells before *in vitro* phosphorylation. These results indicate that MuSK is phosphorylated when overexpressed in a heterologous cell line. Nevertheless, a substantial amount of [^{32}P]phosphate is incorporated into immunoprecipitated MuSK after incubation with [γ-^{32}P]ATP and $MnCl_2$ *in vitro* (Fig. 1*C*). We do not detect other radiolabeled proteins after *in vitro* phosphorylation (Fig. 1*C*), indicating that phosphorylation of MuSK is caused by autophosphorylation rather than phosphorylation by a contaminating kinase present in the MuSK immunoprecipitate.

Mapping of Tyrosine Residues in *in Vitro* Phosphorylated MuSK. After immunoprecipitation and phosphorylation *in vitro*, ^{32}P-labeled MuSK (3–7 μg) was separated by SDS/PAGE and was identified by staining with Coomassie brilliant blue. The MuSK-containing gel slice was incubated with trypsin, and the eluted tryptic peptides were fractionated by reverse phase HPLC on a C18 column. The radioactivity profile shows eight major and four minor peaks (Fig. 1*D*) that were analyzed by MALDI MS; the presence of two peaks of a mass/charge (m/z) difference of 80 indicates the presence of a tyrosine phosphorylated peptide within each fraction. The fragment ion spectra allowed determination of the sequence of phosphorylated peptides. Phosphorylated peptides were identified from all radioactive fractions (Table 1).

We found that 6 of the 19 tyrosine residues in the intracellular region of MuSK were phosphorylated *in vitro* (Fig. 2; Table 1). These include one of the juxtamembrane tyrosine residues

Table 1. Identification of tyrosine-phosphorylated tryptic peptides from *in vitro*-activated MuSK

Fraction no.	Calculated average mass unphosphorylated	Phosphopeptide mass detected	Sequence	Phosphorylated residue
4	901.9	982.5	SHSDLSTR (678–685)	S678
13	1,155.4	1,235.3	LHPNPMYQR (547–555)	Y553
	1,107.2	1,188.2	547–555 with MΔHCSH	Y553
15	1,171.4	1,251.2	LHPNPMoxYQR (547–555)	Y553
21	907.0	987.5	NNIEYVR (572–578)	Y576
26	1,155.4	1,234.7	See fraction 13	Y553
29	1,610.8	1,771.0	DYYKADGNDAIPIR (753–766)	Y754 and Y755
36	1,495.7	1,576.9	YYKADGNDAIPIR (754–766)	Y754
	1,610.8	1,692.3	DYYKADGNDAIPIR (753–766)	Y754
	1,610.8	1,772	753–766, doubly phosphorylated	Y754 and Y755
	1,539.8	1,621	Could correspond to 544–555	Probably Y553
46	1,278.4	1,357.8	AHEEVIYYVR (806–815)	Y812
67	1,439.7	1,519.2	WMPPESIFYNR (767–777)	Y775
69	1,789.9	1,871.2	Probably 806–820	Probably Y812
72	2,410.8	2,491.8	TTLPSELLLDRLHPNPMoxYQR (535–555)	Y553
75	2,394.8	2,474.8	TTLPSELLLDRLHPNPMYQR (535–555)	Y553
77	2,506.3	2,586.7	LTTLPSELLLDRLHPNPMYQR (534–555)	Y553

Fractions collected from the HPLC were analyzed by MALDI MS and were sequenced by PSD. Mox indicates oxidized methionine residues. MΔHCSH indicates a methionine that lost a HCSH group. The masses were determined by measurements in the linear or reflector mode.

Table 2. Identification of tyrosine-phosphorylated tryptic peptides from *in vivo*-activated MuSK

Mass	Sequence	No. of P atoms	Phosphorylated residue
1,215.8	NIYSADYYK	1	Activation loop Y828, Y832, Y833 (Y750, Y754, Y755)
1,295.4	NIYSADYYK	2	
2,310	NIYSADYYKANENDAIPIR	1	
2,390	NIYSADYYKANENDAIPIR	2	
1,235	LHPNPMYQR	1	Juxtamembrane Y631 (Y553 in rat)
1,251	LHPNPMYQR	1	With oxidized M
3,187	TTETPTLATLPSELLLDRLHPNPMYQR	1	
3,203	TTETPTLATLPSELLLDRLHPNPMYQR	1	With oxidized M
986.4	NNIEYVR	1	Beginning of kinase domain Y654 (Y576 in rat)

The peptide mixtures were analyzed by nanoelectrospray tandem mass spectrometry. Phosphorylated peptides were detected by parent ion scans in the negative ion mode.

(Y553) and five tyrosine residues within the kinase domain (Y576, Y754, Y755, Y775, and Y812). Phosphotyrosine residues were detected in multiple peptides because of incomplete cleavage, miscleavage or, chemical modification [especially oxidation of Met residues (see Table 1)].

Peptides containing the activation loop tyrosines, Y754 and Y755, were either monophosphorylated on Y754 or diphosphorylated on Y754 and Y755. Phosphorylation of peptides containing Y812 and Y813 could be unambiguously assigned to Y812 from the PSD spectra. Fraction 4 contained a peptide phosphorylated on serine S678. Phosphorylation of S678 might be catalyzed by a contaminating serine/threonine kinase. Alternatively, S678 phosphorylation may have occurred *in vivo*, and the radioactivity in this early HPLC fraction (5% acetonitrile) may be attributable to a small tyrosine phosphorylated peptide (two to three amino acids) that would be difficult to detect because it would be obscured by the presence of matrix molecules that have a similar mass.

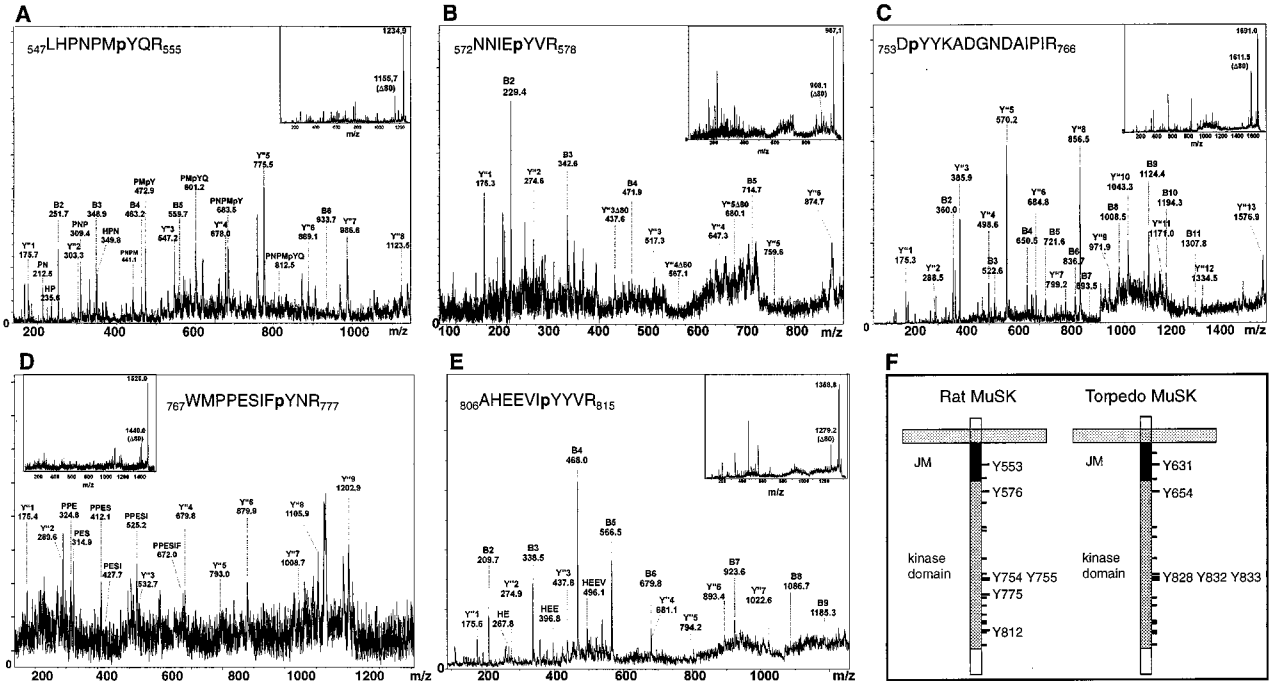

Fig. 2. Fragment ion spectra of phosphopeptides derived from *in vitro* phosphorylated MuSK. The parent ion masses but not the masses of the fragment ions are slightly shifted in some of the PSD spectra. The fragment ions derived from the peptide N-termini (B-ions) and from the C-termini (Y″-ions) are indicated. In some cases, internal fragment ion series derived from proline-directed decay (resulting in a new B-ion series starting from proline) were more prominent than the B-ion series. The inserts show the entire PSD spectra. The regions of the spectra containing the fragment ions are enlarged and annotated. (*A*) pY553. The entire Y″-ion series is apparent in the PSD spectrum, consistent with Y553 as the phosphoamino acid within this peptide. This is further supported by internal fragment ion series starting from P549 and P551. (*B*) pY576. A partial B-ion series and a Y″-ion series. Y″3 containing Y576 is present in the phosphorylated state, indicating that Y576 is the phosphoamino acid within this peptide. Peaks that are not present in a classic ion series are unassigned and most likely arise from cleavage of nonpeptide bonds; their presence does not complicate our ability to assign ions present in a classic series to a particular sequence in MuSK. (*C*) pY754. A prominent B-ion series extending to I764. The B2-ion of 360.0 Da indicates that Y754 is the phosphoamino acid within this peptide. This is supported by the presence of the Y″12-ion containing Y755 in the nonphosphorylated state. (*D*) pY775. Although not all fragment ion signals can be unambiguously interpreted, the Y″-ion series is reliably detected. The peptide sequence is further confirmed by the presence of a partial internal fragment ion series starting from P769. The presence of the Y″-ion series in the phosphorylated state starting from the Y″3-ion indicates that Y775 is the phosphoamino acid within this peptide. (*E*) pY812. The PSD spectrum is dominated by a strong B-ion series. The B7-ion shows up in the phosphorylated state, indicating that Y812 is the phosphoamino acid within this peptide. (*F*) The cartoon illustrates the transmembrane and cytoplasmic domains of rat and *Torpedo* MuSK. The locations of all tyrosine residues are indicated by dashes, and the positions of phosphorylated tyrosine residues are numbered.

Quantitation of the radioactivity profile shows that Y553 is the major phosphorylation site because 58% of the overall radioactivity is incorporated into this residue. The activation loop tyrosines are also major sites of phosphorylation because 26% of the total radioactivity is incorporated into tyrosine residues Y754 and Y755. Y576 (10%) and Y812 (4.5%) are labeled to a lower extent, and Y775 is labeled poorly (1.6%). Because Y812 is located within a large tryptic peptide (residue 778–residue 815; molecular mass = 4,597 Da), which elutes with significantly lower yield from polyacrylamide gels and HPLC columns, it is likely that Y812 is phosphorylated to a greater extent than our calculations suggest. Indeed, we only detect miscleaved smaller peptides containing pY812, indicating that our calculations indeed underrepresent the extent of Y812 phosphorylation. It is likely, however, that we detected all other phosphorylated tyrosine residues because all other tyrosine residues are located in short, hydrophilic tryptic peptides that should be recovered well during the purification procedures.

Nevertheless, to ensure that phosphorylation sites had not been missed because of inefficient elution of peptides from the polyacrylamide gel, we eluted MuSK from the anti-FLAG affinity column with low pH (pH 2.5) and digested MuSK in solution. The radioactivity profile obtained after HPLC separation was identical to that of in-gel digested MuSK, indicating that all tyrosine residues that are phosphorylated *in vitro* were detected by the in-gel digest method (data not shown).

Because some immunoprecipitated MuSK may be misfolded, it is possible that tyrosines that are phosphorylated *in vitro* may not be solvent exposed and phosphorylated *in vivo.* To identify the tyrosines that are phosphorylated *in vivo*, we took advantage of our finding that MuSK is phosphorylated in insect cells. We labeled insect cells with [^{32}P]orthophosphate, immunoprecipitated MuSK, digested MuSK in solution, and fractionated the ^{32}P-labeled peptides by HPLC. The predominant radioactive peaks (fractions 15, 21, 26, 29, and 36 in Fig. 1*D*), corresponding to pY553, pY576, pY754, and pY755, were evident in digests from MuSK labeled *in vivo*. The smaller peaks that eluted later were not as discernible because of the significantly lower incorporation of ^{32}P by labeling *in vivo*. Further, because MuSK was immunoprecipitated but not gel-purified before trypsin cleavage, radiolabeled tryptic fragments derived from minor contaminating proteins increased the background radioactivity and made it difficult to detect minor MuSK tryptic peptides.

Mapping of Phosphorylated Tyrosine Residues in *Torpedo* MuSK *in Vivo.* Finally, we sought to identify the tyrosine residues that are phosphorylated in agrin-activated MuSK *in vivo*. Because MuSK is expressed at low levels in skeletal muscle cells, a substantial amount of [^{32}P]orthophosphate would be required to map the tyrosines that are phosphorylated in agrin-activated MuSK in skeletal muscle cells grown in cell culture. Further, because agrin activates MuSK only in differentiated muscle cells (5), it is not possible to overexpress MuSK in nonmuscle cells and identify tyrosine residues that are phosphorylated by agrin. *Torpedo* electric organ is homologous to skeletal muscle but much more densely innervated; consequently, synaptic proteins, including MuSK, agrin, and AChRs, are expressed at substantially higher levels in the electric organ than in skeletal muscle (11). Therefore, we sought to identify the tyrosine residues that are phosphorylated in endogenous MuSK isolated from the electric organ (Fig. 2*F*).

We immunoprecipitated tyrosine-phosphorylated MuSK (1–3 μg) from the electric organ, fractionated MuSK by SDS/PAGE (Fig. 3*A*), and digested MuSK within the gel slice. The peptides were desalted over a Poros oligoR3 microcolumn and were eluted in three steps. The fractions were analyzed individually by nanoelectrospray tandem mass spectrometry (Fig. 3*B*). The phosphorylated peptides were identified by parent ion scans, which detect

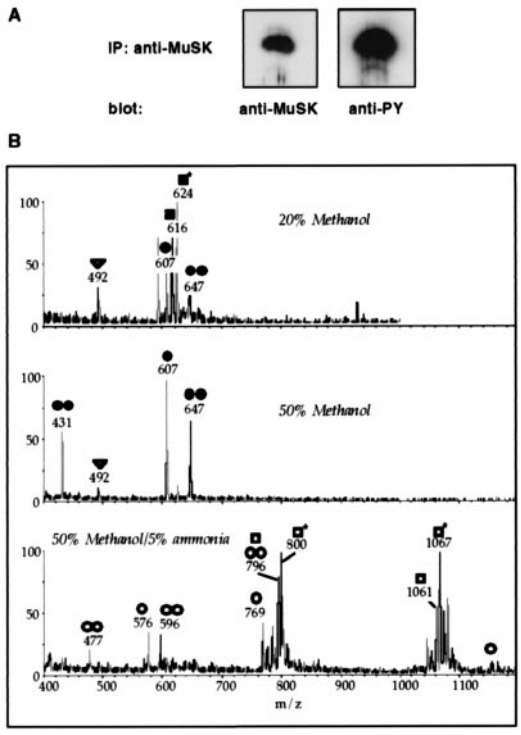

Fig. 3. Mapping of tyrosine phosphorylated residues in *Torpedo* MuSK. (*A*) Immunoprecipitation of activated MuSK from *Torpedo* electric organ. MuSK was immunoprecipitated with antibodies (2847) to MuSK, and Western blots were probed either with antibodies (2847) to MuSK or antibodies to phosphotyrosine (PY, 4G10). (*B*) Parent ion scans detect phosphopeptides in activated MuSK. The digest was analyzed with nanoelectrospray by using parent ion scans of $m/z = 79$ in the negative ion mode for the specific detection of phosphopeptides. (*Top*) Elution of the peptides from the desalting column with 20% methanol. (*Middle*) Elution with 50% methanol. (*Bottom*) Elution with 50% methanol, 5% ammonia. The following peptides were detected: ●, 1,216 Da (826–834) + 1P; ●●, 1,295 (826–834) + 2P; ○, 2,310 Da (826–844) + 1P; ○○, 2,390 Da (826–844) + 2P; ■, 1,235 Da (625–633) + 1P; ■*, 1,251 (625–633) + 1P (oxidized methionine); □, 3,187 Da (607–633) + 1P; □*, 3,203 Da (607–633) + 1P (oxidized methionine); ▽, 986 Da (650–656) + 1P.

peptides that produce a distinct fragment ion on collision-induced dissociation. In the case of phosphorylated peptides, the fragment ion is PO_3^- with $m/z = 79$ detected in the negative ion mode. For two of the peptides (650–656 and 607–633), the phosphorylated amino acids could be determined by mass spectrometric sequence determination (data not shown).

As summarized in Table 2, we found phosphorylated tryptic peptides containing the juxtamembrane tyrosine residue Y631 (Y553 in rat), with or without oxidized methionine. Phosphorylated tryptic peptides containing the activation loop tyrosines Y828, Y832, and Y833 (Y750, Y754, and Y755 in rat) were detected with either one, two, or three phosphorylated tyrosine residues. Further, we also detected a phosphorylated tryptic peptide containing tyrosine Y654 (Y576 in rat). These results indicate that the juxtamembrane tyrosine, the activation loop tyrosines, and the tyrosine residue near the N-terminal end of the kinase domain are phosphorylated in endogenous MuSK *in vivo*. The residue corresponding to Y775 in rat MuSK is a phenylalanine in *Torpedo* MuSK. Peptides containing pY890 (Y812 in rat) were not detected in *Torpedo* MuSK digested with trypsin. This peptide may have escaped detection because of a low level of phosphorylation and/or reduced extraction and detection efficiency of this relatively large peptide (4.5 kDa). Nevertheless, the high sensitivity of precursor ion scans and the ability to detect peptides as large as 6 kDa with this method

(unpublished data) raise the possibility that phosphorylation of Y812 *in vitro* is caused by partial unfolding of MuSK or inappropriate *in vitro* labeling conditions.

Discussion

Agrin stimulates the rapid phosphorylation of MuSK leading to clustering of synaptic proteins at the neuromuscular junction. In a first step to elucidate the signal transduction cascade downstream from MuSK, we identified tyrosine residues that are phosphorylated in activated MuSK and that might serve as docking sites for proteins with SH2- or PTB-domains.

Activation Loop Tyrosines. Three tyrosine residues, Y750, Y754, and Y755, are contained within the activation loop of the MuSK kinase domain. Most tyrosine kinases have either one (homologous to Y754), two (homologous to Y754 and Y755), or three tyrosine residues in their activation loop. Phosphorylation of these tyrosines in other RTKs results in a shift of an inhibitory domain and a substantial increase in kinase activity (18).

We found peptides containing tyrosine residues Y754 and Y755 either mono- or diphosphorylated in the *in vitro* experiments. Monophosphorylated peptides were phosphorylated on Y754. Phosphorylation of the third tyrosine residue of the activation loop, Y750, was not detected *in vitro*. In the *in vivo* experiments, however, we detected a tryptic peptide in which all three activation loop tyrosines were phosphorylated. These results are in good agreement with studies of the insulin receptor in which the tyrosine corresponding to Y750 is phosphorylated only at high concentrations of ATP and is the last of the three activation loop tyrosines to be phosphorylated (18, 19). Consistent with our biochemical data showing that each of the activation loop tyrosines are phosphorylated *in vivo*, mutation of the activation loop tyrosines of MuSK results in a failure of agrin to activate MuSK in muscle cells grown in cell culture (20).

Juxtamembrane Tyrosine Y553. The juxtamembrane tyrosine residue is the predominant phosphorylation site in MuSK activated *in vitro*. These results are consistent with studies showing that Y553 is essential for MuSK signaling (20, 21). The juxtamembrane tyrosine residue is located within an NPXY motif that can serve as a docking site for PTB domain-containing proteins. Because interactions with PTB domain-containing proteins can be phosphorylation-dependent (7), phosphorylation of Y553 may serve as a key regulatory step in initiating a signaling cascade downstream from MuSK (20).

Y576 and Y812. Phosphorylation of Y576 and Y812 is unexpected. Phosphorylation of Y576, however, is unlikely to be spurious because phosphorylation of Y576 is detected both *in vitro* and *in vivo*. Further, although no other RTK contains a tyrosine residue at the position corresponding to Y576, both Y576 and Y812 are conserved in MuSK from all classes sequenced to date. Both the incorporation of ^{32}P as well as the ready detection of the corresponding peptide in precursor ion scans indicates that Y576 is phosphorylated to a substantial degree *in vitro* and *in vivo*. Moreover, the location of this residue within the β1-sheet in the N-terminal lobe of the kinase domain, which should be accessible for interacting proteins, indicate that this residue might serve as a docking site for SH2-domain-containing proteins. The sequences adjacent to pY576 and pY812, however, do not conform to binding-sites for known SH2 domain-containing proteins. Importantly, functional studies demonstrate that Y576 indeed has a role in agrin-mediated signaling because agrin induces fewer AChR clusters in MuSK mutant muscle cells expressing Y576F MuSK than wild-type MuSK (20). Our data indicate that the failure of agrin to stimulate phosphorylation of Y576 in these cells is responsible for their defect in AChR clustering.

The significance of Y812 phosphorylation is more difficult to assess. Phosphorylation of Y812 was detected *in vitro* and in insect cells but not in endogenous MuSK isolated from *Torpedo* electric organ. Our inability to confirm phosphorylation of Y812 in MuSK isolated from *Torpedo* electric organ may be attributable to the large mass of the Y812-containing tryptic peptide, which is likely to be recovered in poor yield. Nevertheless, mutational studies indicate that mutation of Y812 does not reduce the ability of agrin to stimulate clustering of AChRs (20). Because MuSK activation *in vivo* regulates multiple aspects of postsynaptic differentiation and presynaptic differentiation (3), it is possible, however, that phosphorylation of Y812 is required for other aspects of synaptic differentiation.

Other Tyrosine Residues. A sixth tyrosine residue, Y775, is phosphorylated *in vitro*. Because this tyrosine is not conserved in *Torpedo*, we do not know whether this tyrosine is phosphorylated *in vivo* by agrin. The low level of phosphorylation of Y775 *in vitro* as well as the fact that this tyrosine is not conserved in *Torpedo* MuSK imply that this tyrosine is either not phosphorylated *in vivo* or its phosphorylation is not required for MuSK function.

The tyrosine residue corresponding to Y831 in MuSK is phosphorylated in other RTKs, including Trks (22), and has been reported to serve as a docking site for the p85 subunit of phosphatidylinositol 3-kinase (PI3-kinase) (23). We do not detect phosphorylation of Y831 either *in vitro* or *in vivo*. Considering the high sensitivity of the nanoelectrospray- and MALDI MS (within the femtomole range for the parent ion scans), it is unlikely that Y831 is phosphorylated in activated MuSK. Further, it is unlikely that agrin stimulates phosphorylation of Y831 and activates PI3-kinase because (*i*) mutation of Y831 has no effect on agrin-induced clustering of AChRs (20, 21), (*ii*) agrin fails to stimulate phosphorylation of p85, and (*iii*) wortmanin, an inhibitor of PI3-kinase, fails to block agrin-stimulated clustering of AChRs (20).

This work was supported by a postdoctoral fellowship from the Deutsche Forschungsgemeinschaft to A.W. and a research grant from the National Institutes of Health (Grant NS 36193) to S.J.B.

1. Glass, D. J. & Yancopoulos, G. D. (1997) *Curr. Opin. Neurobiol.* **7,** 379–384.
2. Burden, S. J. (1998) *Genes Dev.* **12,** 133–148.
3. DeChiara, T. M., Bowen, D. C., Valenzuela, D. M., Simmons, M. V., Poueymirou, W. T., Thomas, S., Kinetz, E., Compton, D. L., Rojas, E., Park, J. S., *et al.* (1996) *Cell* **85,** 501–512.
4. Sanes, J. R. & Lichtman, J. W. (1999) *Annu. Rev. Neurosci.* **22,** 389–442.
5. Glass, D. J., Bowen, D. C., Stitt, T. N., Radziejewski, C., Bruno, J., Ryan, T. E., Gies, D. R., Shah, S., Mattsson, K., Burden, S. J., *et al.* (1996) *Cell* **85,** 513–523.
6. Pawson, T. (1995) *Nature (London)* **373,** 573–580.
7. van der Geer, P., Hunter, T. & Lindberg, R. A. (1994) *Annu. Rev. Cell Biol.* **10,** 251–337.
8. Kalo, M. S. & Pasquale, E. B. (1999) *Biochemistry* **38,** 14396–14408.
9. Carr, S. A., Huddleston, M. J. & Annan, R. S. (1996) *Anal. Biochem.* **239,** 180–192.
10. Neubauer, G. & Mann, M. (1999) *Anal. Chem.* **71,** 235–242.
11. Jennings, C. G., Dyer, S. M. & Burden, S. J. (1993) *Proc. Natl. Acad. Sci. USA* **90,** 2895–2899.
12. Harlow, E. & Lane, D. L. (1988) *Antibodies: A Laboratory Manual* (Cold Spring Harbor Lab. Press, Plainview, NY).
13. Valenzuela, D. M., Stitt, T. N., DiStefano, P. S., Rojas, E., Mattsson, K., Compton, D. L., Nunez, L., Park, J. S., Stark, J. L., Gies, D. R., *et al.* (1995) *Neuron* **15,** 573–584.
14. Laemmli, U. K. (1970) *Nature (London)* **227,** 680–685.
15. Shevchenko, A., Wilm, M., Vorm, O. & Mann, M. (1996) *Anal. Chem.* **68,** 850–858.
16. Wilm, M., Neubauer, G. & Mann, M. (1996) *Anal. Chem.* **68,** 527–533.
17. Dreger, M., Otto, H., Neubauer, G., Mann, M. & Hucho, F. (1999) *Biochemistry* **38,** 9426–9434.
18. Hubbard, S. R., Wei, L., Ellis, L. & Hendrickson, W. A. (1994) *Nature (London)* **372,** 746–754.
19. Hubbard, S. R., Mohammadi, M. & Schlessinger, J. (1998) *J. Biol. Chem.* **273,** 11987–11990.
20. Herbst, R. & Burden, S. J. (2000) *EMBO J.* **19,** 67–77.
21. Zhou, H., Glass, D. J., Yancopoulos, G. D. & Sanes, J. R. (1999) *J. Cell Biol.* **146,** 1133–1146.
22. Stephens, R. M., Loeb, D. M., Copeland, T. D., Pawson, T., Greene, L. A. & Kaplan, D. R. (1994) *Neuron* **12,** 691–705.
23. Obermeier, A., Lammers, R., Wiesmuller, K. H., Jung, G., Schlessinger, J. & Ullrich, A. (1993) *J. Biol. Chem.* **268,** 22963–22966.